

Enhanced Catalytic Ozonation by Mn–Ce Oxide-Loaded Al_2O_3 Catalyst for Ciprofloxacin Degradation

Dajie Yang, Fanbin Meng, Zhuoran Zhang, and Xiang Liu*

Cite This: *ACS Omega* 2023, 8, 21823–21829

Read Online

ACCESS |



Metrics & More

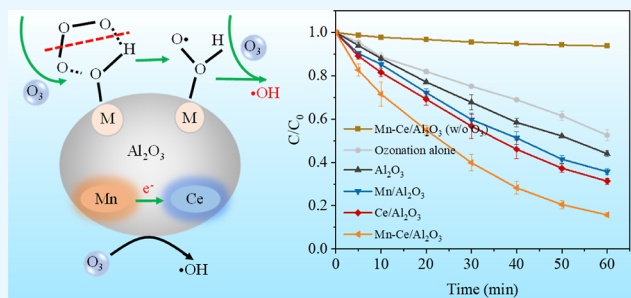


Article Recommendations



Supporting Information

ABSTRACT: Catalytic ozonation is an effective and promising advanced oxidation technology for organic pollutant removal. Herein, $\text{Ce}_x\text{Mn}_{1-x}\text{O}_2$ metal oxides loaded on Al_2O_3 catalysts (Mn–Ce/ Al_2O_3) were synthesized for catalytic ozonation of the wastewater containing ciprofloxacin. The morphology, crystal structure, and specific surface area of the prepared catalyst were characterized. The characteristics of the Mn–Ce/ Al_2O_3 catalyst revealed that the loaded MnO_2 could interfere with the formed CeO_2 crystals and then produced complex $\text{Ce}_x\text{Mn}_{1-x}\text{O}_2$ oxides. Compared with an ozone-alone system (47.4%), the ciprofloxacin degradation efficiency in the Mn–Ce/ Al_2O_3 catalytic ozonation system elevated to 85.1% within 60 min. The ciprofloxacin degradation kinetic rate over the Mn–Ce/ Al_2O_3 catalyst is 3.0 times that of the ozone-alone system. The synergetic corporation of redox pairs between Mn(III)/Mn(IV) and Ce(III)/Ce(IV) in the Mn–Ce/ Al_2O_3 catalyst could accelerate ozone decomposition to generate active oxygen species and further significantly improve the mineralization efficiency of ciprofloxacin. The work demonstrates the great potential of developing dual-site ozone catalysts for advanced treatment of wastewater.



1. INTRODUCTION

Ciprofloxacin is widely used as an antibiotic, which can inhibit the growth of both Gram-positive and Gram-negative bacteria.^{1–3} After being metabolized by humans or animals, more than 50% of ciprofloxacin will be excreted with feces and urine in the form of antibiotics itself and its metabolites into the wastewater system.⁴ Unfortunately, the detection concentration of antibiotics in the tail-water of wastewater treatment plants indicates that the conventional wastewater treatment process is not effective for ciprofloxacin removal.⁵ As a result, ciprofloxacin is widespread in surface waters. Considering the potential adverse effects of ciprofloxacin on the ecological environment, there is an urgent need to develop an efficient wastewater treatment technology for ciprofloxacin removal.

Recently, the catalytic ozonation technology has been considered as an effective technology for refractory organic pollutant treatment. Especially, heterogeneous catalytic ozonation could improve the mass-transfer efficiency of ozone from the gas phase to the liquid phase and accelerate O_3 decomposition into hydroxyl radicals ($\cdot\text{OH}$).^{6–8} The advantages of catalytic ozonation, such as high oxidation efficiency and reusability of the catalyst, make it to be a potential and environmentally friendly ozone treatment method for wastewater treatment. Due to the important role of catalyst materials in affecting catalytic oxidation efficiency,⁹ intensive research has been conducted to design efficient catalysts for catalytic ozonation.

Due to the large specific surface area, mesoporous structure, high hardness, and high mechanical strength, the activated alumina-supported metal catalyst is one of the most used components in the field of catalytic ozonation process.^{10–13} Especially, transitional-metal oxides, such as Fe, Cu, Mn, and Ce oxides, displayed great potential for ozone decomposition and reactive oxygen species (ROS) generation, subsequently improving the degradation efficiency of the organic pollutants.^{14–16} Compared with single-component metal-loaded catalysts, the construction of multiple metal-loaded catalysts may achieve the synergetic effect among the active components for the catalytic ozonation process. The development of the multiple metal-loaded catalysts is of great significance for the catalytic ozonation technology in treating antibiotic-containing wastewater.

In this work, a highly efficient and stable multiple metal-loaded alumina catalyst Mn–Ce/ Al_2O_3 was prepared and ciprofloxacin was selected as a typical quinolone antibiotic pollutant. The catalytic ozonation performance of Mn–Ce/ Al_2O_3 for ciprofloxacin degradation was tested. The

Received: March 6, 2023

Accepted: May 16, 2023

Published: June 5, 2023



physicochemical properties of the catalysts were investigated to explore the relationship between the structure properties and catalytic activity. The catalytic mechanism of treating wastewater containing ciprofloxacin by catalytic ozonation with Mn–Ce/Al₂O₃ was revealed.

2. EXPERIMENTAL SECTION

2.1. Experimental Materials. Ciprofloxacin and ciprofloxacin-D8 were purchased from Tianjin Alta Scientific Co., Ltd. Activated alumina was purchased from Shanghai Macklin Biochemical Co., Ltd. Both cerium nitrate and manganese nitrate were produced by Sinopharm Group Chemical Reagent Co., Ltd. All chemical reagents were used without any further purification. The water used in the experimental process was deionized water. All pieces of glassware were washed with deionized water several times before use and dried in a 105 °C oven.

2.2. Preparation of Catalysts. **2.2.1. Activation Treatment of Al₂O₃ Microspheres.** The activated alumina microspheres (Φ 3–5 mm) with uniform shape were selected and washed three times with deionized water to remove the residual impurities and dust on the surfaces of particles and then dried in an oven at 110 °C for 10 h. Dried activated alumina microspheres were transferred to a muffle furnace, calcined at 400 °C for 3 h, and then cooled to room temperature and stored for future use.

2.2.2. Preparation of the Loaded Activated Al₂O₃ Catalyst. A certain amount of activated Al₂O₃ microspheres were put into 0.5 mol L⁻¹ manganese nitrate, cerium nitrate, and manganese nitrate–cerium nitrate mixed solution (the molar concentration ratio of manganese nitrate to cerium nitrate was set to 1:1). The suspension was placed in a conical flask and then vibrated in a shaker for 6 h to achieve the adsorption equilibrium. After filtration, activated Al₂O₃ microspheres were placed in an oven at 60 °C for drying and then placed in a muffle furnace and calcined at 500 °C for 3 h to obtain metal oxide-loaded Al₂O₃ catalysts. Three catalysts with different components were prepared under the same conditions and labeled as Mn/Al₂O₃, Ce/Al₂O₃, and Mn–Ce/Al₂O₃.

2.3. Catalyst Characterization. The microscopic morphology of the catalysts was analyzed by scanning electron microscopy (SEM). The crystal structure of the metal-loaded-activated Al₂O₃ catalysts was analyzed by X-ray diffraction (XRD). The elemental composition and its chemical state on the catalyst surface were analyzed by X-ray photoelectron spectrometry (XPS). The specific surface area and pore size distribution were determined with the Brunauer–Emmett–Teller method and Barrett–Joyner–Halenda method using a specific surface area analyzer. The surface charge of the catalysts and the zero charge pH point (pH_{zpc}) were determined using a Zeta potential meter. The hydroxyl radical (•OH) generation was identified by a Bruker ER073 spectrometer (Karlsruhe, Germany) using 5,5-dimethylpyridine-*N*-oxide (DMPO) as the spin-trapping reagent. *tert*-Butanol was employed as an •OH scavenger to verify the contribution of •OH to the degradation of ciprofloxacin.

2.4. Catalytic Ozonation of Ciprofloxacin. A 15 L of simulated wastewater containing ciprofloxacin (5.0 mg L⁻¹) and a certain mass of solid catalyst were added into a reactor and evenly mixed by the magnetic stirrer. The ozone generator was used to provide O₃ (Figure S1 in the Supporting Information). After a certain reaction time, water samples

were taken out and 0.5 mL of Na₂S₂O₃ solution (0.01 mol L⁻¹) was added dropwise to terminate the ozonation reaction. After the catalyst in the water sample was precipitated, the supernatant was taken for ciprofloxacin detection. In the ozone-alone experiment, no solid catalyst was added into the reactor. In the catalyst adsorption experiment, oxygen was directly introduced into the reactor without opening the ozone generator, while other experimental conditions were kept the same as the catalytic ozonation experiment.

3. RESULTS AND DISCUSSION

3.1. Morphology and Structure Characterization. The surface structure of the catalyst would affect not only the diffusion process of pollutants on the surface but also the exposure of the surface active sites.¹⁷ Figure 1 shows SEM

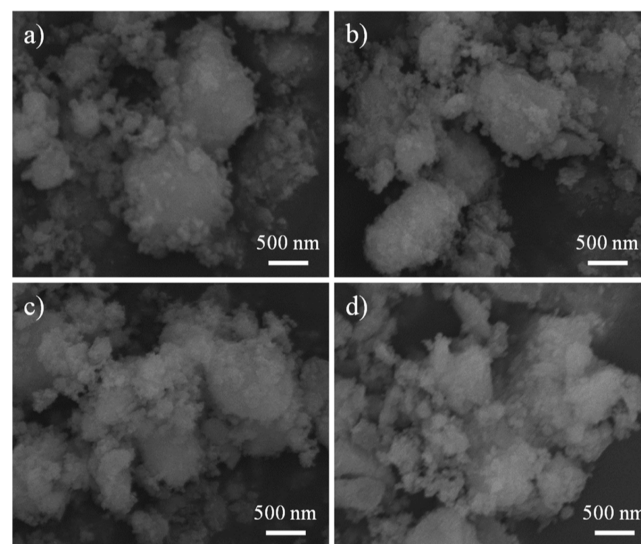


Figure 1. SEM images of the prepared catalysts. (a) Al₂O₃ microspheres, (b) Mn/Al₂O₃, (c) Ce/Al₂O₃, and (d) Mn–Ce/Al₂O₃.

images of the prepared catalysts. The surface of the Al₂O₃ microsphere displays irregular morphology, which is mainly due to the inhomogeneous packing of Al₂O₃ particles on the surface. The pores in the Al₂O₃ microsphere would facilitate the diffusion of ozone molecules or organic molecules into the interior of Al₂O₃ microspheres. Compared to the bare Al₂O₃ catalyst, some dispersed nanoparticles were displayed on the surface of Mn/Al₂O₃, Ce/Al₂O₃, and Mn–Ce/Al₂O₃ catalysts, which should be the formed MnO₂ or CeO₂ nanoparticles. When Al₂O₃ microspheres were immersed into a metal nitrate solution, metal ions would get adsorbed on the surface of Al₂O₃ particles. After the high-temperature calcination, the metal nitrates were further converted into metal oxide particles and tightly fixed on the surface of the activated Al₂O₃ particles.

The XRD spectra of the prepared Al₂O₃ catalysts are shown in Figure 2. The active Al₂O₃ exhibits characteristic diffraction peaks at 38.7 and 67.3° (Standard Card PDF#80-0956). After loading metal oxides, the Mn/Al₂O₃ catalyst exhibits the characteristic diffraction peak of MnO₂ at 37.5° (Standard Card PDF#44-0141). The curve of the Ce/Al₂O₃ catalyst shows the characteristic peaks of CeO₂ at 28.5 and 47.5° (standard card PDF#43-1002), indicating that manganese nitrate and cerium nitrate have been converted into MnO₂ or CeO₂ nanoparticles after the impregnation-calcination process.^{18,19}

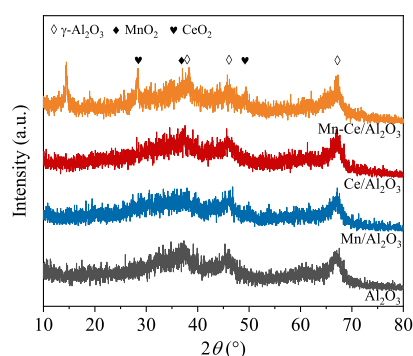


Figure 2. XRD patterns of the metal-loaded Al_2O_3 catalyst.

The XPS spectra of metal-supported active Al_2O_3 catalysts are shown in Figure 3. It can be seen that the Mn–Ce/ Al_2O_3 catalyst shows characteristic peaks of Al 2p, O 1s, Mn 2p, and Ce 3d, demonstrating that Mn and Ce species have been successfully loaded in the activated Al_2O_3 catalyst. For Mn/ Al_2O_3 and Mn–Ce/ Al_2O_3 catalysts, the Mn 2p spectrum presents two sets of characteristic peaks at 642.1 and 653.2 eV, corresponding to Mn 2p_{1/2} and Mn 2p_{3/2}, respectively. Using the Gaussian fitting, the Mn 2p_{3/2} peaks could be fitted to the characteristic energies of 642.2 and 643.5 eV, corresponding to Mn (III) and Mn (IV), respectively.²⁰ These results indicate that Mn oxides mainly exist in the form of MnO_2 , with a small amount present in the form as Mn (III).

Due to the high localization of 4f electrons in CeO_2 nanocrystals, it is easy to form oxygen vacancies on CeO_2 surfaces in Ce/ Al_2O_3 and Mn–Ce/ Al_2O_3 catalysts, which further induces the part reduction of Ce(IV) to Ce(III). The high-resolution XPS curve to the Ce 3d XPS spectrum was further fitted with Gaussian curves; 10 spin–orbit peaks appeared, in which *v* represented the split peak generated by the Ce 3d_{3/2} spin–orbit and *u* represented the split peak generated by the Ce 3d_{5/2} spin–orbit.^{21,22} Table 1 lists the binding energy positions where different splitting peaks appeared, among which Ce (III) exhibited a quadruple split peak structure, corresponding to *v*₀, *v*₁, *v*₂, and *v*₃, respectively. Ce(IV) exhibited a sixfold split peak structure, corresponding to *v*₄, *v*₅, *u*₀, *u*₁, *u*₂, and *u*₃, respectively. The ratio of Ce(III)/Ce(IV) can be estimated in terms of the peak areas.²³ The results show that the atomic ratios of Ce(III)/Ce(IV) in Ce/ Al_2O_3 and Mn–Ce/ Al_2O_3 catalysts are 0.79 and 0.83,

respectively. Indeed, the Ce (III) content in Ce oxides plays an important role in determining the catalytic performance.

The specific surface area of the catalyst is closely related to the exposed active sites, which in turn affects the catalyst activity. Figure 4 shows the N_2 adsorption–desorption isotherms of the Al_2O_3 , Mn/ Al_2O_3 , Ce/ Al_2O_3 , and Mn–Ce/ Al_2O_3 catalysts. The activated Al_2O_3 microspheres have a relatively large specific surface area ($289.1 \text{ m}^2 \text{ g}^{-1}$). The loading of active metal components does not significantly affect the specific surface area of Al_2O_3 microspheres. There are large numbers of mesoporous structures in the catalyst with pore size mainly varying from 3 to 10 nm (Table 2). These porous structures in the microspheres would facilitate the diffusion and adsorption of ozone and organic pollutants into the catalyst and subsequently enhance the interaction between ozone molecules and the catalytic active sites.

3.2. Catalytic Ozonation Performance toward Ciprofloxacin. Ciprofloxacin was selected as the model pollutant to investigate the catalytic ozonation degradation performance of the metal-supported active Al_2O_3 catalysts. Before the catalytic degradation experiment, the adsorption abilities of active Al_2O_3 , Mn/ Al_2O_3 , Ce/ Al_2O_3 , and Mn–Ce/ Al_2O_3 catalysts to ciprofloxacin were investigated. It indicated that the adsorbed amount of ciprofloxacin by all catalysts is <3% within 30 min, indicating that the adsorption capacities of the prepared Al_2O_3 catalyst are weak. Figure 5 shows the ciprofloxacin degradation curves in different catalytic ozonation systems. In the ozone-alone system, about 47% ciprofloxacin was degraded in 60 min. The introduction of Al_2O_3 catalysts improved the ciprofloxacin degradation efficiency (56%), indicating that the Al_2O_3 catalyst could enhance the catalytic ozonation reaction. Al_2O_3 microspheres are beneficial to the transfer of ozone molecules at the solid–liquid interface, and then the Lewis acidic sites on Al_2O_3 surface could serve as active sites for catalyzing ozone decomposition to generate ROS.

However, the catalytic ozonation efficiency of the Al_2O_3 catalyst is low. After loading the active metal components, the degradation efficiency of ciprofloxacin on Mn/ Al_2O_3 , Ce/ Al_2O_3 , and Mn–Ce/ Al_2O_3 catalysts reached 65, 69, and 85%, respectively, within 60 min. The degradation curves of ciprofloxacin were fitted by the first-order kinetic equation, which fitted well with the pseudo-first-order kinetic process. The degradation rate constant of ciprofloxacin was 0.0102 min^{-1} in the ozone-alone system. The presence of Al_2O_3 catalysts accelerates the ciprofloxacin degradation rate (0.0135 min^{-1}). Compared with the single-metal-loaded Mn/

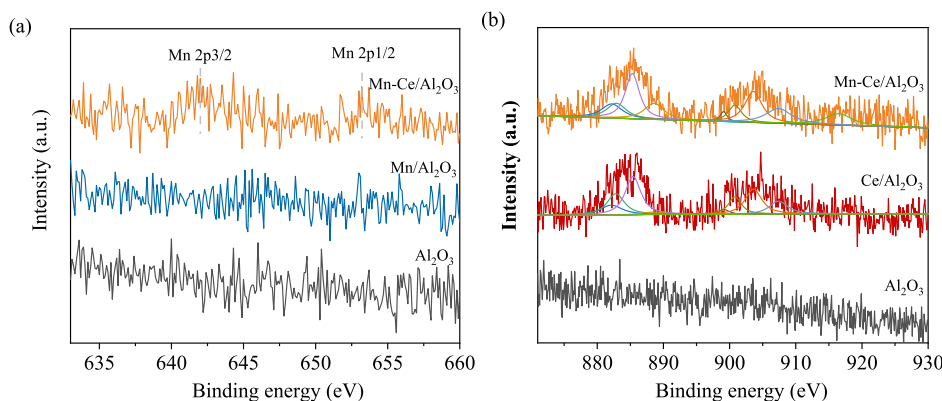
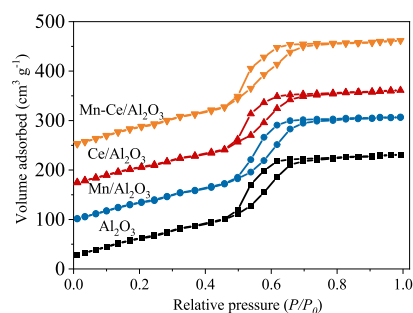


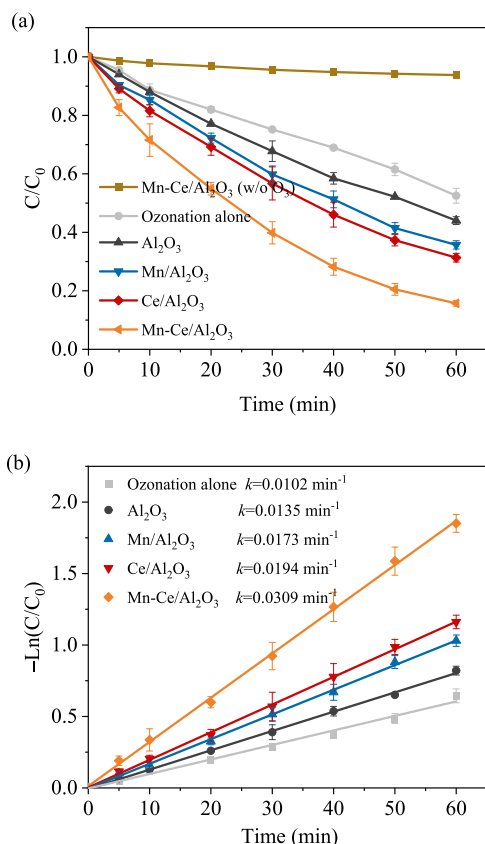
Figure 3. High-resolution XPS spectra of (a) Mn 2p and (b) Ce 3d for the metal-loaded Al_2O_3 catalyst.

Table 1. Energy Positions of Ce 3d_{3/2} and Ce 3d_{5/2} Spin–Orbit Components

sample name	ν_0	ν	ν'	ν''	ν'''	u_0	u	u'	u''	u'''
Ce/Al ₂ O ₃	882.1	882.8	885.4	888.6	898.0	899.1	900.8	903.6	907.4	916.5
Mn–Ce/Al ₂ O ₃	882.2	882.9	885.3	888.9	898.3	899.4	901.0	903.4	907.3	916.4

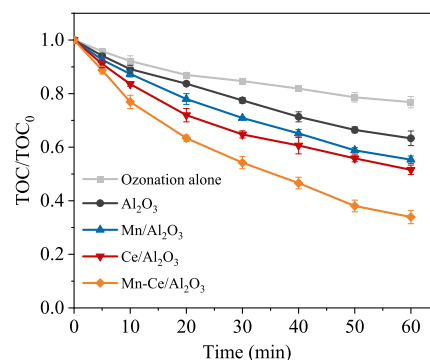
**Figure 4.** N₂ adsorption–desorption isotherms of different Al₂O₃ catalysts.**Table 2. Surface Area, Pore Diameter, and Pore Volume of Different Catalysts**

sample name	specific surface area (m ² g ⁻¹)	pore size (nm)	pore volume (cm ³ g ⁻¹)	pHzpc
Al ₂ O ₃	289.1	5.63	0.46	7.3
Mn/Al ₂ O ₃	281.3	6.50	0.48	5.3
Ce/Al ₂ O ₃	273.4	5.92	0.51	6.9
Mn–Ce/Al ₂ O ₃	280.9	6.20	0.49	6.6

**Figure 5.** (a) Degradation performance of ciprofloxacin during the catalytic ozonation over different Al₂O₃-based catalysts and (b) the corresponding pseudo-first-order reaction kinetic analysis. ([ciprofloxacin] = 5 mg L⁻¹, [catalyst] = 10.0 g L⁻¹, pH = 6.40).

Al₂O₃ or Ce/Al₂O₃ catalysts, the Mn–Ce/Al₂O₃ catalyst further improved the ciprofloxacin degradation rate, which was 3.0 times (0.0309 min⁻¹) that of the ozone-alone system, indicating that loading of bimetallic active components remarkably improves the catalytic ozonation performance of activated Al₂O₃.

Figure 6 shows the mineralization efficiency curves of ciprofloxacin in different catalyst systems. In the ozone-alone

**Figure 6.** Mineralization performance of ciprofloxacin during the catalytic ozonation over different Al₂O₃-based catalysts ([ciprofloxacin] = 5 mg L⁻¹, [catalyst] = 10.0 g L⁻¹, pH = 6.40).

system, the removal efficiency of total organic carbon (TOC) was 23% at 60 min, indicating that the single ozonation system has limited ability to mineralize ciprofloxacin due to the generation of intermediates. The introduction of Al₂O₃, Mn/Al₂O₃, and Ce/Al₂O₃ catalysts significantly improved the mineralization efficiency of ciprofloxacin. Especially, TOC removal efficiency of ciprofloxacin over the Mn–Ce/Al₂O₃ catalyst reached 67% at 60 min, which should be attributed to the fact that the Mn–Ce/Al₂O₃ catalyst could greatly catalyze and decompose ozone molecules to generate reactive oxygen radicals.

3.3. Optimization of Catalyst Preparation Conditions.

The composition of the prepared catalyst determines the content of active components in Al₂O₃ support, which in turn affects its catalytic ozonation performance. Figure 7 displays the effect of precursor concentration on the performance of the Mn–Ce/Al₂O₃ catalyst for ozonation degradation of ciprofloxacin. With the increase of active component concentration in the impregnation solution, the ciprofloxacin degradation on Mn–Ce/Al₂O₃ shows a trend of increasing first and then decreasing, which can be attributed to the lack of sufficient sites at low loadings and the pore-clogging on Al₂O₃ microsphere surface at high loadings. The highest degradation efficiency of ciprofloxacin on the Mn–Ce/Al₂O₃ catalyst occurred at an active component concentration of 0.5 mol L⁻¹. Thus, proper catalyst composition in the Mn–Ce/Al₂O₃ catalyst is important to promote the catalytic ozonation performance.

The effect of the initial pH value of the reaction solution on the catalytic ozonation performance of the Mn–Ce/Al₂O₃ catalyst was further investigated. As shown in Figure 8, the

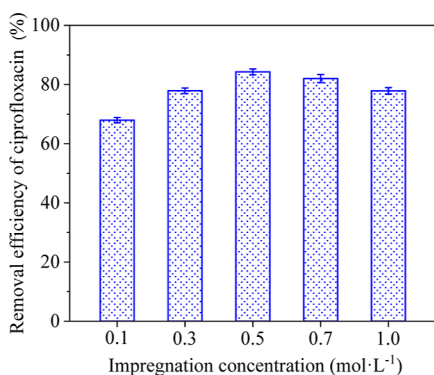


Figure 7. Ciprofloxacin degradation efficiency over the Mn–Ce/Al₂O₃ catalyst prepared at different impregnation concentrations ([ciprofloxacin] = 5 mg L⁻¹, [catalyst] = 10.0 g L⁻¹, pH = 6.40).

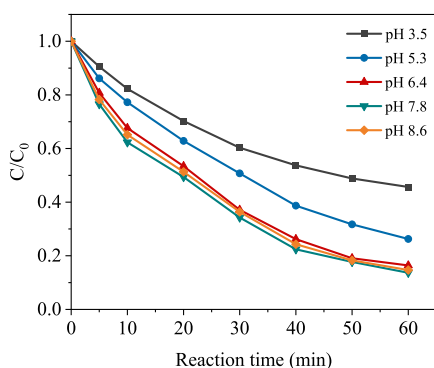


Figure 8. Effect of solution pH on ciprofloxacin removal efficiency in the Mn–Ce/Al₂O₃ catalytic ozonation process.

removal efficiencies of ciprofloxacin were 54.3, 73.7, 83.5, 86.3, and 85.1% within 60 min at the initial pH of the reaction solution of 3.5, 5.3, 6.4, 7.8, and 8.6, respectively. It can be observed that the degradation efficiency of ciprofloxacin significantly increases as the initial pH value increases. The catalytic ozonation degradation efficiency of ciprofloxacin under neutral and alkaline conditions is much higher than that under acidic conditions. This can be attributed to the increased –OH groups on Mn–Ce/Al₂O₃ catalyst surface at high solution pH, which can act as the active sites for catalyzing ozone decomposition.

3.4. Stability of Mn–Ce/Al₂O₃ Catalyst. The stability of the catalyst during the catalytic process is critical in a heterogeneous catalysis reaction. To investigate the stability of the Mn–Ce/Al₂O₃ catalyst during catalytic ozonation, the cyclic catalytic ozonation degradation experiments were conducted (Figure 9). The performance of the Mn–Ce/Al₂O₃ catalyst for catalytic ozonation degradation of ciprofloxacin was not significantly reduced after five repeated cycles. In the fifth repeated experiment, the degradation efficiency of ciprofloxacin still reached >80%, indicating that the prepared Mn–Ce/Al₂O₃ catalyst has good stability during the catalytic ozonation process. In addition, the dissolution of Mn and Ce ions on the catalyst surface during the catalytic ozonation process was further measured (Table 3). After the reaction, the dissolved concentration of Mn and Ce ions in the solution was lower than 0.01 mg L⁻¹. These results indicate that the synthesized Mn–Ce/Al₂O₃ catalyst possesses good stability and reusability, which is of great importance for the engineering applications of the catalytic ozonation technology.

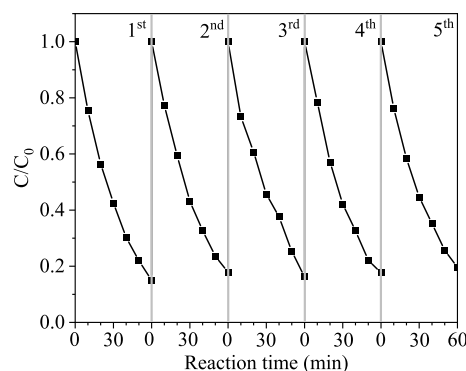


Figure 9. Cycling runs of the Mn–Ce/Al₂O₃ catalyst for the catalytic ozonation degradation of ciprofloxacin.

Table 3. Dissolution of Metal Ions during the Catalytic Ozonation Degradation of Ciprofloxacin by the Mn–Ce/Al₂O₃ Catalyst

the reused times	Mn ion concentration (mg L ⁻¹)	Ce ion concentration (mg L ⁻¹)
1	0.0042	0.0024
2	0.0031	0.0017
3	0.0035	0.0019
4	0.0016	0.0016
5	0.0021	0.0012

3.5. Reaction Mechanism Analysis of Catalytic Ozonation. Since the adsorption of ciprofloxacin over different metal-supported active Al₂O₃ catalysts was less than 5%, it is concluded that most of the degradation of ciprofloxacin was completed by catalytic ozonation pathways. Electron spin resonance (ESR) spectroscopy was used to verify the produced ROS during the catalytic ozonation process.²⁴ DMPO was used as the spin capture reagent to detect the generated •OH radicals. As shown in Figure 10a, a typical four-line characteristic signal of DMPO–•OH (1:2:2:1) was clearly observed, which demonstrates the generation of •OH in the catalytic ozonation system. Compared to the Al₂O₃ catalyst system, the significantly enhanced DMPO–•OH signal in the Mn–Ce/Al₂O₃ catalyst system suggests the promoted ozone decomposition and ROS generation, which would enhance the degradation of ciprofloxacin in wastewater.

To determine the critical active species during ciprofloxacin degradation, radical quenching experiments were further performed. As shown in Figure 10b, the degradation efficiency of ciprofloxacin was greatly inhibited in the presence of *tert*-butyl alcohol (•OH scavenger) in the Mn–Ce/Al₂O₃ catalyst system. This result suggests that •OH plays an important role in promoting ciprofloxacin degradation. According to the analysis of the free-radical capture experiment and free-radical quenching experiment, the enhanced generation of OH in the Mn–Ce/Al₂O₃ system mainly contributes to ciprofloxacin degradation.

Based on the above results, the mechanism of the catalytic ozonation reaction over the Mn–Ce/Al₂O₃ catalyst is proposed as follows (Figure 11). The hydroxyl group on the catalyst surface plays an important role in the ozone decomposition.^{25,26} In the aqueous environment, the water molecules coordinate with Lewis acid on the Mn–Ce/Al₂O₃ catalyst surface, and then water molecules dissociate and form hydroxyl groups and H⁺ on the catalyst surface. The highly

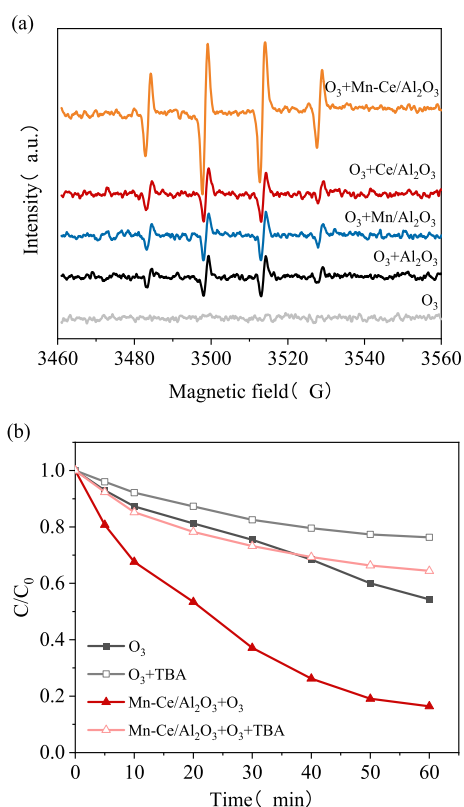


Figure 10. (a) ESR spectra of the DMPO-•OH adduct recorded at 5 min over different catalytic ozonation systems. (b) Effect of *tert*-butyl alcohol on ciprofloxacin removal efficiency over different catalytic ozonation systems.

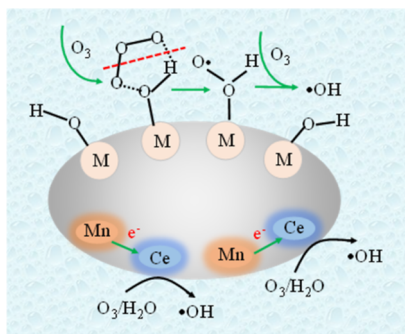
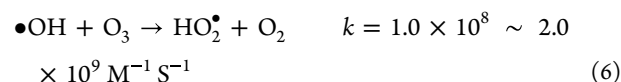
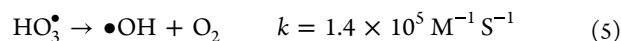
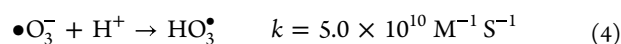
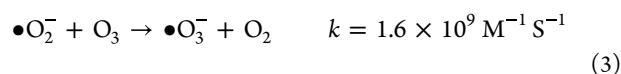
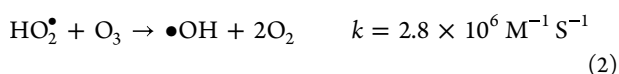
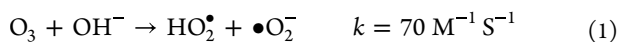


Figure 11. Schematic representation of the zone oxidation reaction on Mn-Ce/Al₂O₃ catalyst surface.

active surface resonance structure of ozone molecules makes it coordinate with the hydroxyl group on Mn-Ce/Al₂O₃ catalyst surface to form a five-membered ring structure, which subsequently induces the coordination structure to release O₂ molecules and generate •O₂H or •O₂⁻ on catalyst surface. Meanwhile, ozone molecules and •O₂H- would generate •OH through a series of reactions and then achieve oxidative degradation of ciprofloxacin molecules to achieve wastewater purification (eqs 1–6)



4. CONCLUSIONS

The multiple activated metal component catalyst Mn-Ce/Al₂O₃ was successfully prepared by an impregnation-calcination method for catalytic ozonation degradation. The Mn-Ce/Al₂O₃ catalyst exhibited superior catalytic performance, resulting in 85% degradation of ciprofloxacin within 60 min. The degradation kinetic constant with Mn-Ce/Al₂O₃ is 3.0, 1.8, and 1.6 times than that with the ozone-alone system, Mn/Al₂O₃ system, and Ce/Al₂O₃ system, respectively. Although there is a direct oxidation process by ozone molecules in both the ozone-alone system and Mn-Ce/Al₂O₃ catalytic system, Mn-Ce/Al₂O₃ catalyst could more efficiently catalyze the decomposition of ozone to generate reactive oxygen radicals, which significantly improves the mineralization efficiency of ciprofloxacin. The synergetic corporation of bimetallic active components Mn(III)/Mn(IV) and Ce(III)/Ce(IV) in the Mn-Ce/Al₂O₃ catalyst could promoted the catalytic ozone decomposition and subsequently enhance ROS generation in the catalytic ozonation process for ciprofloxacin degradation. The highly catalytic ozonation performance Mn-Ce/Al₂O₃ will help the development of a high-efficiency ozone catalytic oxidation system to achieve the effective degradation of antibiotics in water and high purification of reclaimed water.

■ ASSOCIATED CONTENT

Supporting Information

The Supporting Information is available free of charge at <https://pubs.acs.org/doi/10.1021/acsomega.3c01302>.

Schematic diagram of the experimental apparatus for catalytic ozonation (PDF)

■ AUTHOR INFORMATION

Corresponding Author

Xiang Liu – School of Environment, Tsinghua University, Beijing 10084, China; Email: x.liu@tsinghua.edu.cn

Authors

Dajie Yang – School of Environment, Tsinghua University, Beijing 10084, China; Ministry of Water Resources, Beijing 10053, China; orcid.org/0009-0002-7156-7955
 Fanbin Meng – SINOPEC Research Institute of Petroleum Processing Co., Ltd., Beijing 100083, China
 Zhuoran Zhang – School of Environment, Tsinghua University, Beijing 10084, China

Complete contact information is available at:

<https://pubs.acs.org/doi/10.1021/acsomega.3c01302>

Notes

The authors declare no competing financial interest.

ACKNOWLEDGMENTS

This work was supported by the Open Foundation of Beijing Key Laboratory of Water Environmental and Ecological Technology for River Basins (BKL-KF-2021-001-SZY).

REFERENCES

- (1) De Witte, B.; Dewulf, J.; Demeestere, K.; Van Langenhove, H. Ozonation and advanced oxidation by the peroxone process of ciprofloxacin in water. *J. Hazard. Mater.* **2009**, *161*, 701–708.
- (2) Rocha, D. C.; da Silva Rocha, C.; Tavares, D. S.; de Moraes Calado, S. L.; Gomes, M. P. Veterinary antibiotics and plant physiology: an overview. *Sci. Total Environ.* **2021**, *767*, 144902.
- (3) Zhang, G. F.; Liu, X.; Zhang, S.; Pan, B.; Liu, M. L. Ciprofloxacin derivatives and their antibacterial activities. *Eur. J. Med. Chem.* **2018**, *146*, 599–612.
- (4) Hayes, A.; May Murray, L.; Catherine Stanton, I.; Zhang, L.; Snape, J.; Hugo Gaze, W.; Kaye Murray, A. Predicting selection for antimicrobial resistance in UK wastewater and aquatic environments: Ciprofloxacin poses a significant risk. *Environ. Int.* **2022**, *169*, 107488.
- (5) Qalyoubi, L.; Al-Othman, A.; Al-Asheh, S. Removal of ciprofloxacin antibiotic pollutants from wastewater using nano-composite adsorptive membranes. *Environ. Res.* **2022**, *215*, 114182.
- (6) Vittenet, J.; Aboussaoud, W.; Mendret, J.; Pic, J.-S.; Debellefontaine, H.; Lesage, N.; Faucher, K.; Manero, M. H.; Thibault-Starzyk, F.; Leclerc, H.; et al. Catalytic ozonation with γ - Al_2O_3 to enhance the degradation of refractory organics in water. *Appl. Catal., A* **2015**, *504*, 519–532.
- (7) Ikhlaq, A.; Brown, D. R.; Kasprzyk-Hordern, B. Mechanisms of catalytic ozonation on alumina and zeolites in water: Formation of hydroxyl radicals. *Appl. Catal., B* **2012**, *123–124*, 94–106.
- (8) Yu, D.; Wu, M.; Hu, Q.; Wang, L.; Lv, C.; Zhang, L. Iron-based metal-organic frameworks as novel platforms for catalytic ozonation of organic pollutant: Efficiency and mechanism. *J. Hazard. Mater.* **2019**, *367*, 456–464.
- (9) Nawrocki, J.; Kasprzyk-Hordern, B. The efficiency and mechanisms of catalytic ozonation. *Appl. Catal., B* **2010**, *99*, 27–42.
- (10) Bing, J.; Hu, C.; Zhang, L. Enhanced mineralization of pharmaceuticals by surface oxidation over mesoporous γ - $\text{Ti-Al}_2\text{O}_3$ suspension with ozone. *Appl. Catal., B* **2017**, *202*, 118–126.
- (11) Nawaz, F.; Cao, H.; Xie, Y.; Xiao, J.; Chen, Y.; Ghazi, Z. Selection of active phase of MnO_2 for catalytic ozonation of 4-nitrophenol. *Chemosphere* **2017**, *168*, 1457–1466.
- (12) Wu, M.; Wang, X.; Dai, Q.; Li, D. Catalytic combustion of chlorobenzene over $\text{Mn-Ce}/\text{Al}_2\text{O}_3$ catalyst promoted by Mg. *Catal. Commun.* **2010**, *11*, 1022–1025.
- (13) Wang, Z.; Li, C.; Guo, Y.; Cheng, J.; Song, Z.; Sun, D.; Qi, F.; Ikhlaq, A. Model prediction and mechanism analysis of PPCPs abatement in secondary effluent by heterogeneous catalytic ozonation: A case study with $\text{MnO}_2\text{-Co}_3\text{O}_4$ depends on DOM concentration. *Chem. Eng. J.* **2023**, *455*, 140792.
- (14) Ma, N.; Ru, Y.; Weng, M.; Chen, L.; Chen, W.; Dai, Q. Synergistic mechanism of supported Mn–Ce oxide in catalytic ozonation of nitrofurazone wastewater. *Chemosphere* **2022**, *308*, 136192.
- (15) Ma, N.; Ru, Y.; Weng, M.; Chen, L.; Chen, W.; Dai, Q. Synergistic mechanism of supported Mn–Ce oxide in catalytic ozonation of nitrofurazone wastewater. *Chemosphere* **2022**, *308*, 136192.
- (16) Liu, H.; Gao, Y.; Wang, J.; Pan, J.; Gao, B.; Yue, Q. Catalytic ozonation performance and mechanism of $\text{Mn-CeO}_x/\gamma\text{-Al}_2\text{O}_3/\text{O}_3$ in the treatment of sulfate-containing hypersaline antibiotic wastewater. *Sci. Total Environ.* **2022**, *807*, 150867.
- (17) Wang, Y.; Yu, G. Challenges and pitfalls in the investigation of the catalytic ozonation mechanism: A critical review. *J. Hazard. Mater.* **2022**, *436*, 129157.
- (18) Li, P.; Zhan, S.; Yao, L.; Xiong, Y.; Tian, S. Highly porous alpha- MnO_2 nanorods with enhanced defect accessibility for efficient catalytic ozonation of refractory pollutants. *J. Hazard. Mater.* **2022**, *437*, 129235.
- (19) Wang, D.; He, Y.; Chen, Y.; Yang, F.; He, Z.; Zeng, T.; Lu, X.; Wang, L.; Song, S.; Ma, J. Electron transfer enhancing the Mn(II)/Mn(III) cycle in MnO/CN towards catalytic ozonation of atrazine via a synergistic effect between MnO and CN. *Water Res.* **2023**, *230*, 119574.
- (20) Gao, E.; Meng, R.; Jin, Q.; Yao, S.; Wu, Z.; Li, J.; Du, E. Highly effective mineralization of acetic acid wastewater via catalytic ozonation over the promising $\text{MnO}_2/\gamma\text{-Al}_2\text{O}_3$ catalyst. *Chem. Phys. Impact* **2023**, *6*, 100149.
- (21) Wang, J.; Quan, X.; Chen, S.; Yu, H.; Liu, G. Enhanced catalytic ozonation by highly dispersed CeO_2 on carbon nanotubes for mineralization of organic pollutants. *J. Hazard. Mater.* **2019**, *368*, 621–629.
- (22) Zhang, X.; Xu, Z.; Jiang, M.; Chen, S.; Han, Z.; Liu, Y.; Liu, Y. Enhanced activity of CuO_y/TNTs doped by CeO_x for catalytic ozonation of 1,2-dichloroethane at normal temperatures: Performance and catalytic mechanism. *Sep. Purif. Technol.* **2023**, *311*, 123255.
- (23) Ma, N.; Ru, Y.; Weng, M.; Chen, L.; Chen, W.; Dai, Q. Synergistic mechanism of supported Mn–Ce oxide in catalytic ozonation of nitrofurazone wastewater. *Chemosphere* **2022**, *308*, 136192.
- (24) Qi, F.; Chen, Z.; Xu, B.; Shen, J.; Ma, J.; Joll, C.; Heitz, A. Influence of surface texture and acid–base properties on ozone decomposition catalyzed by aluminum (hydroxyl) oxides. *Appl. Catal., B* **2008**, *84*, 684–690.
- (25) Joseph, C. G.; Farm, Y. Y.; Taufiq-Yap, Y. H.; Pang, C. K.; Nga, J. L. H.; Li Puma, G. Ozonation treatment processes for the remediation of detergent wastewater: A comprehensive review. *J. Environ. Chem. Eng.* **2021**, *9*, 106099.
- (26) Rekhate, C. V.; Srivastava, J. K. Recent advances in ozone-based advanced oxidation processes for treatment of wastewater- A review. *Chem. Eng. J. Adv.* **2020**, *3*, 100031.